# Comparison of the Electrical, Optical, and Electrochemical Properties of Diamond and Indium Tin Oxide Thin-Film Electrodes

**ARTICLE** *in* CHEMISTRY OF MATERIALS · AUGUST 2005

Impact Factor: 8.35 · DOI: 10.1021/cm050762z



**4 AUTHORS**, INCLUDING:

Greg M Swain
Michigan State University
**177** PUBLICATIONS **5,588** CITATIONS

SEE PROFILE

# Comparison of the Electrical, Optical, and Electrochemical Properties of Diamond and Indium Tin Oxide Thin-Film Electrodes

Jason Stotter, Yoshiyuki Show, Shihua Wang, and Greg Swain*

*Department of Chemistry and the Fraunhofer Center for Coatings and Laser Applications, Michigan State University, East Lansing, Michigan 48824*

*Received April 9, 2005. Revised Manuscript Received July 15, 2005*

The electrical, optical, and electrochemical properties of an optically transparent diamond electrode are reported on and compared with those of a commonly used optically transparent electrode (OTE), indium tin oxide (ITO). The OTE was formed by coating a thin film (ca. 0.5−1 $\mu$m) of boron-doped diamond on quartz. The electrode possesses an electrical resistivity of $10^{-2}$ Ω cm, or less, and an optical transparency of ca. 55% between 300 and 900 nm. The properties were evaluated before and after 48 h exposure tests to different organic solvents (hexane, toluene, methanol, and dichloromethane) and aggressive aqueous solutions (1 M $HNO_3$ and 1 M NaOH) and 2 h electrochemical polarizations in the same aqueous media. In contrast to ITO, the electrical and optical properties of the diamond OTE were stable during all the aqueous solution and organic solvent soak tests and during 2 h electrochemical polarizations at maximum anodic and cathodic current densities of ≥5 mA/cm$^2$. The electrochemical properties of the diamond OTE were also unaffected by soak tests or electrochemical polarization. For example, cyclic voltammetric $\Delta E_p$ values of 86 mV for $Fe(CN)_6^{3-/4-}$ and 67 mV for $Ru(NH_3)_6^{3+/2+}$ were observed prior to and remained unchanged after 1 h polarizations in strong acid and base. Electrochemical atomic force microscopy (ECAFM) was used to explore the diamond and ITO surface morphology during anodic and cathodic polarization. No structural changes were observed for diamond while extensive surface roughening was seen for ITO, consistent with microstructural alterations. Finally, the homogeneity of the diamond OTE's electrical properties was probed by conductivity-probe atomic force microscopy (CPAFM). It was observed that the film consists of isolated regions of high electrical conductivity separated by zones of lower conductivity.

## Introduction

Spectroelectrochemical measurements in the UV−vis region of the electromagnetic spectrum involve recording changes in the optical properties of a redox analyte, either dissolved in solution or confined to a surface, as a function of a change in its oxidation state brought about by heterogeneous electron-transfer with an electrode.[1,2] Over the past four decades, UV-Vis spectroelectrochemistry has become an essential tool in the study of redox processes particularly when the processes are reversible and the reactants or products are optically active. Transmission is the simplest measurement mode in which an electrode functions both as an optical window transparent to the electromagnetic radiation of interest and as a source or sink for electrons. Such a material is known as an optically transparent electrode (OTE). Through the years, metal (Au, Pt), carbon, and metal oxide thin films, coated on glass or quartz, have been used as OTEs for UV−vis spectroelectrochemical measurements. Of these, the indium tin oxide (ITO) films have been the most studied. ITO is a tin (Sn(IV))-doped, $In_2O_3$-based *n-type* semiconductor. It and ZnO have been extensively investigated over the past 20 years for application in electrooptical devices and photovoltaics.[4] Our interest is in the use of OTE's for transmission spectroelectrochemical measurements. Reproducibile and stable electrical, optical, and electrochemical properties are reqirements for an OTE in such measurements.

Transmission spectroelectrochemical measurements using a new type of carbon OTE, boron-doped diamond thin film, have been reported on recently.[5−8] Several architectures have been investigated so far including a thin film of diamond deposited on quartz that is transparent in the UV−vis,[6] a thin film of diamond deposited on Si that is transparent in the IR,[5,7] and a free-standing diamond disk that is transparent in both the UV−vis and IR.[5,7] The usefulness of the free-standing diamond disk and the diamond thin film on quartz for transmission spectroelectrochemical studies has been demonstrated for $Fe(CN)_6^{3-/4-}$, methyl viologen, ferrocene, chlorpromazine, and cytochrome *c*.[5−8] In related work, Martin and Morrison reported on a study of the carbon−oxygen

* To whom correspondence should be addressed. E-mail: swain@chemistry.msu.edu.

(1) Kuwana, T.; Darlington, R. K.; Leedy, D. W. *Anal. Chem.* **1964**, *36*, 2023−2025.
(2) Kuwana, T.; Winograd, N. In *Electroanalytical Chemistry*; Bard, A. J., Ed.; Marcel Dekker: New York, 1974; Vol. 7, p 2.
(3) Crayston, J. A. In *Encyclopedia of Electrochemistry (Instrumentation and Electroanalytical Chemistry)*; Unwin, P., Ed.; Wiley-VCH: Weinheim, Germany, 2003; Vol. 3, p 491.
(4) Ginley, D. S.; Bright, C. *MRS Bull.* **2000**, *8*, 15.
(5) Zak, J. K.; Butler, J. E.; Swain, G. M. *Anal. Chem.* **2001**, *73*, 908.
(6) Stotter, J.; Zak, J. K.; Behler, Z.; Show, Y.; Swain, G. M. *Anal. Chem.* **2002**, *74*, 5924.
(7) Haymond, S.; Zak, J. K.; Show, Y.; Butler, J. E.; Babcock, G. T.; Swain, G. M. *Anal. Chim. Acta* **2003**, *500*, 137.
(8) Stotter, J.; Haymond, S.; Zak, J.; Show, Y.; Cvacková, Z.; Swain, G. M. *Interface* **2003**, *12*, 33.

10.1021/cm050762z CCC: $30.25 
Published on Web 00/00/0000 PAGE EST: 8.2

functional groups introduced on the diamond surface during anodic polarization using an internal reflection IR spectroelectrochemical measurement.[9] The focus of our work, most recently, has been on the growth and characterization of thin-film diamond coated on quartz. This OTE possesses (i) an electrical resistivity of $10^{-2}$ Ω cm or less and an optical transparency of ca. 55% between 300 and 900 nm, (ii) a working potential window of 3 V or more in aqueous media, (iii) a low and stable background current, (iv) relatively rapid electron-transfer kinetics for some redox systems without conventional pretreatment, and (v) weak molecular adsorption of polar molecules (i.e., deactivation and fouling resistance).[10]

Diamond is a wide band gap semiconductor and, therefore, possesses optical transparency in the visible and IR regions of the electromagnetic spectrum. A key issue with making a transparent diamond electrode is balancing the boron-doping level to impart sufficient electrical conductivity while maintaining optical transparency. While previous work has shown that this new type of carbon OTE can function in spectroelectrochemical measurements, there has been no comprehensive study of the electrical, optical, and electrochemical properties and how they are affected during use. The optical and electrical properties of diamond and ITO have been compared to some extent in a previous publication, but not in a comprehensive manner.[6]

The purpose for this manuscript is to comprehensively report on the electrical, optical, and electrochemical properties of the diamond OTE in comparison with ITO. Details of the film growth procedure are first given. This is followed by a discussion of the electrical and optical properties of the two electrode materials before and after exposure to different organic solvents and aggressive aqueous solutions and electrochemical polarization in the same aqueous media. The electrochemical properties of the two electrodes before and after the solution exposure tests and the electrochemical polarization are then described. Electrochemical atomic force microscope images are presented which further demonstrate the stability of the diamond morphology during electrochemical polarization. Finally, results from conductivity-probe atomic force microscopy measurements are presented which reveal heterogeneities in the electrical conductivity across the diamond OTE surface.

## Experimental Section

**Deposition of Thin-Film Diamond on Quartz.** Boron-doped diamond was deposited on quartz, as described previously.[6] The quartz was prepared for growth by, first, introducing many fine scratches on the surface by polishing with a 0.1 μm diamond powder slurrried in ultrapure water on a felt polishing cloth. The polishing debris and excess diamond powder were then removed by extensive ultrasonic cleaning in acetone and solvent rinsing. This cleaning is a critical step in the process. The clean scratches and adventitiously embedded diamond particles serve as the initial nucleation sites for diamond growth. A high density of scratches and embedded particles leads to the formation of a thin and continuous film because of a high instantaneous nucleation density. The resulting film is composed of small crystallites of relatively uniform diameter. A source gas mixture of 0.5% (v/v) $CH_4$ in $H_2$ was employed for the deposition. The source gas also contained 10 ppm $B_2H_6$ for boron doping. Growth was carried out at a system pressure of 45 Torr, a microwave power of 600 W, and a growth temperature of ca. 800 °C. The last step in the deposition process was a short, postgrowth anneal in an $H_2$ plasma (45 Torr, 600 W) to remove adventitious nondiamond $sp^2$ carbon impurity and to fully hydrogen terminate the surface. The coated substrate was then cooled to below 400 °C in the presence of atomic hydrogen by gradually reducing the pressure and power over a 5−10 min period to 25 and 300 W, respectively. The resulting films were ca. 500 nm thick (1 h growth) with a nominal electrical resistivity of 0.06 Ω cm or less as measured with a four-point tungsten probe.

**ITO Electrodes.** Commercial ITO, sputter-deposited on a fused quartz slides, was used (CQ-90IN, Delta Technologies, Ltd, Stillwater, MN). The films were deposited from a target having a 90−10 In/Sn atomic ratio. The film thickness was reported by the manufacturer to be 200 nm, and the sheet resistance was given as 100 Ω/sq. The electrical resistivity, as measured in our laboratory using a four-point probe, was nominally about $3 \times 10^{-5}$ Ω cm. Individual ITO/quartz samples were cut into 1 $cm^2$ pieces by scoring along the uncoated surface and breaking. A film was used after rinsing with ultrapure water and distilled 2-propanol. Films from three different batches were evaluated.

**Solution Exposure Tests.** Electrode soak tests were performed for 48 h at room temperature in toluene (MCB Manufacturing Chemists, Inc., ACS), hexane (Baker, ACS, 97%), methanol (Baker, ACS, 99.8%), dichloromethane (Mallinckrodtkt, ACS), 1 M $HNO_3$ (Cleveland Chemical Industries, 70% ACS), and 1 M NaOH (Spectrum, ACS). The aqueous solutions were prepared with ultrapure water from a Barnstead E-Pure system. The organic solvents were used as received. A different electrode was used for testing in each liquid. A transmission spectrum in the UV−vis region and an in-plane resistivity measurement were made for each film before and after exposure.

**UV−Vis Transmission Measurements.** A transmission spectrum was recorded after rinsing a film with ultrapure water and distilled 2-propanol and drying under a stream of $N_2$. A plastic mask and holder, shaped to fit into the cuvette holder of a commercial UV−vis spectrophotometer (Shimadzu UV2401-PC), was used to position the samples in the optical path. The light was incident on the film side of the quartz. The electrode was placed over an opening in the mask and secured in place with double-sided adhesive tape. The electrode remained attached to the mask during the electrochemical polarization to ensure that the spectra were collected from the treated region. All transmission spectra were recorded against air in the reference beam path. The refractive indices of diamond, quartz, and air were assumed to be 2.41, 1.54, and 1.00, respectively.

**Electrical Measurements.** The electrical resistivity was measured with an tungsten tip, four-point probe (in-line arrangement) connected to an analogue multimeter (HP 3478A, Hewlett-Packard, Palo Alto, CA), which was operated in a four-wire resistance measurement mode. The probe spacing was 0.1 cm. A constant current was applied between the other two probes, and the voltage drop between the inner two probes was measured. The measured resistance, $R$, from the $I-V$ data was converted to a resistivity, $\rho$, according to the equation

$$\rho(\Omega\ \mathrm{cm}) = 4.532 l R(\Omega)$$

where $l$ is the film thickness (cm). Multiple measurements were usually made at different locations on a film.

(9) Martin, H. B.; Morrison, P. W. *Electrochem. Solid-State Lett.* **2001**, *4*, E17.
(10) Xu, J.; Chen, Q.; Swain, G. M. *Anal. Chem.* **1998**, *70*, 3146.

**Electrochemical Polarization.** The diamond OTE was polarized by sweeping the potential between the oxygen and hydrogen evolution regions at 25 mV/s over a 2 h period in 1 M $HNO_3$ and 1 M NaOH (>28 cycles). The potential limits used were −1.5 and +2.5 V in acid and −2.0 and +2.0 V in base. The reference was a commercial Ag/AgCl electrode filled with 4 M KCl saturated with AgCl (0.197 V vs NHE). The maximum current at the potential limits was ±1 mA (±5 mA/cm$^2$) or greater. ITO was polarized by sweeping the potential between the oxygen and hydrogen evolution regions at 25 mV/s until electrical contact with the film was lost, which usually occurred within the first 10−20 cycles (vide infra). The potential limits used were −1.0 and +2.5 V in acid and −1.7 and +1.7 V in base. The maximum currents at the potential limits were ±1 mA (±5 mA/cm$^2$) or greater.

**Electrochemical Measurements.** Electrochemical measurements were made using a computer-controlled potentiostat (model 1200, Cypress Systems, Inc., Lawrence, KS) in a standard, three-electrode configuration.[11] The electrode was clamped to the bottom of a single compartment, glass electrochemical cell. A Viton O-ring (i.d. 0.5 cm) placed between the cell opening and the electrode surface ensured that a reproducible area of 0.2 cm$^2$ was exposed to the electrolyte solution. Contact with the diamond was made by pressing a piece of nickel foil against the entire film surface outside the O-ring. A neoprene rubber spacer was cut to the same dimensions of the nickel foil and used to force the foil into contact with the electrode surface. Contact with the ITO was made by attaching a smooth metal clip to a portion of the conductive surface outside the O-ring. The O-ring was sonicated for 10 min in ultrapure water, rinsed with distilled 2-propanol (IPA), and dried with a stream of $N_2$ before use. Once mounted in the cell, the electrode was cleaning by soaking in distilled 2-propanol (IPA) for 20 min and then rinsed thoroughly with distilled water.[12] The cell was then filled with the electrolyte solution of interest. Nitrogen was bubbled through the solution for 10 min to remove dissolved oxygen, and the solution was blanketed with the gas during the entirety of a measurement. The auxiliary electrode was a large-area carbon rod that was rinsed with distilled IPA and dried with $N_2$ between measurements. The reference was a commercial Ag/AgCl electrode filled with 4 M KCl saturated with AgCl (0.197 V vs NHE). The reference electrode was placed in a cracked-glass capillary filled with the supporting electrolyte and positioned near the working electrode.

**Optical Microscopy.** Optical micrographs were captured using an Olympus metallurgical microscope (Scope BX60M, Olympus America, Inc., Melville, NY) fitted with a digital camera (DP11, Olympus America, Inc., Melville, NY). Images were collected using an optical polarization filter to highlight the different domains in a film.

**Electrochemical Atomic Force Microscopy (EC-AFM) Measurements.** Scanning probe microscopy was performed using a Nanoscope IIIa multimode microscope (Digital Instruments/Veeco Metrology Group, Santa Barbara, CA). Double-sided tape was used to affix an electrode to the magnetic disk sample holder, which held the sample in place on the piezo scanner. Electrical connection between the ITO surface and the magnetic disk was made with Ag paint applied to the corners of the square sample. Electrical connection with the conductive diamond surface was made with fine wire affixed to the corners by conductive tape. A small volume of the electrolyte solution was then placed in the fluid cell using a syringe. An Ag wire served as a quasi-reference electrode (Ag QRE), and a coiled Pt wire was used as the counter electrode. The reference and counter electrodes were inserted into the electrolyte solution through separate ports in the fluid cell. The electrolyte solution was replaced periodically during the electrochemical polarizations due to the gas buildup that occurred at the positive and negative potential limits. The pyramidal $Si_3N_4$ probe tips were used with 200 $\mu$m narrow-leg cantilevers having a spring constant of 0.06 N/m. The film roughness was estimated using the root-mean-square (rms) roughness calculation script available in the image analysis software. Both electrode surfaces were generally smooth, so the roughness calculation was performed without the use of any plane fitting scripts.

**Conductivity-Probe Atomic Force Microscopy (CP-AFM).** CP-AFM measurements were made with a NanoScope IIIa multimode microscope, a Signal Access Module, and a laboratory-built current−voltage converter with gain. A gold-coated $Si_3N_4$ tip was used to make contact with the electrode surface (NPG-20, Veeco, Santa Barbara, CA). Current−position profiles were obtained using a +2.0 V bias between the sample and tip. A current−voltage converter with amplification was used to convert the current flowing through the tip into a proportional voltage for output to the Signal Access Module. This voltage was recorded at each point across the surface simultaneously with a height-mode topographical scan.

## Results and Discussion

**Electrical and Optical Properties of Diamond and ITO.** Results from this and prior work have revealed that the electrical properties of the diamond OTE are quite stable during exposure of a variety of organic solvents (hexane, toluene, methanol, and dichloromethane) and aggressive aqueous solutions (1 M $HNO_3$ and 1 M NaOH).[6] For example, one set of diamond thin films examined in this work possessed an electrical resistivity that was nominally $4 \times 10^{-2}$ Ω cm before and increased, at most, to $6 \times 10^{-2}$ Ω cm after exposure to any of the solvents or solutions. Clearly, the electrical properties of diamond are unaffected during exposure to all the different organic and aqueous media, and this is because of the material's microstructural stability, strong adhesion with the quartz, and resistance to chemical attack.

The electrical properties of ITO were also found to be stable during exposure to hexane, toluene, or methanol. However, the resistivity increased by many orders of magnitude after exposure to dichloromethane. This was caused by localized film dissolution, as evidenced by optical microscopy. Mixed results were seen for ITO during exposure to 1 M $HNO_3$ or 1 M NaOH. For one batch of electrodes, no change in the electrical properties was observed after exposure to either solution. However, for another batch, significant increases (several orders of magnitude) in the film resistivity were noted after exposure to either solution, similar to what was reported previously.[6] The increased resistivity was caused, at least in part, by localized chemical attack and film dissolution, as revealed by optical microscopy. The instability of ITO in these aggressive aqueous solutions, particularly mineral acid, is recognized and has been noted before.[13] The fact that some films were stable while others were not must be related to a variable

(11) Granger, M. C.; Witek, M.; Xu, J.; Wang, J.; Hupert, M.; Hanks, A.; Koppang, M. D.; Butler, J. E.; Lucazeau, G.; Mermoux, M.; Strojek, J. W.; Swain, G. M. *Anal. Chem.* **2000**, *72*, 3793.

(12) Ranganathan, S.; Kuo, T.-C.; McCreery, R. L. *Anal. Chem.* **1995**, *67*, 3574.

(13) Armstrong, N. R.; Lin, A. W. C.; Fujihira, M.; Kuwana, T. *Anal. Chem.* **1976**, *48*, 741.

morphology or film thickness from batch to batch. For instance, a batch with a thicker and more defect-free coating would require more time for chemical attack and complete removal from the substrate than would a thinner, more defective film.

Important, though, is the fact that the electrical resistivity of ITO is lower than that for diamond by 2−3 orders of magnitude. Application of OTE's in organic light-emitting diodes and flat panel displays, for example, require the lowest possible electrical resistivity to overcome problems of device response time and series resistance.[14−17] The electrical resistivity of a material is directly related to the charge carrier concentration and the carrier mobility. For diamond, the primary source of charge carriers is the substitutionally inserted boron.[18−20] In the case of ITO, the free carriers originate from two principal donors: Sn(IV) substituting in the crystalline lattice for In and doubly charged oxygen vacancies. Hall measurement data have been reported for crystalline and amorphous films of ITO. Typical carrier concentrations for the more crystalline films are in the $10^{20}-10^{21}$ $cm^{-3}$ range, and carrier mobilities are in the 10−50 $cm^2/(V\ s)$ range.[14,15] Preliminary Hall measurement data have also been obtained for the diamond OTE (van der Paaw contact arrangement). Typical carrier concentrations are in the $10^{20}-10^{21}$ $cm^{-3}$ range also, but the carrier mobilities are lower by about 2 orders of magnitude, in the 0.1−1 $cm^2/(V\ s)$ range.[6] The lower carrier mobility in the nanograined diamond is the reason for the higher electrical resistivity. The abrupt grain boundaries in the material reduce the carrier velocity laterally through a film, as the carriers are believed to be moving through both the grains and grain boundaries of the film. It is because of the low carrier mobility that the lower limit of the electrical resistivity seems to be in the $10^{-3}$ Ω cm range. The low electrical resistivity of this particular batch of ITO is realized because of a high carrier mobility. The high mobility probably results from the crystalline, rather than amorphous, nature of the microstructure. While the higher resistivity of the diamond OTE would be a drawback for electrooptical applications, its is sufficiently low for electrochemcial measurements, under normal conditions, to be made relatively free from ohmic resistance effects. In other words, the higher electrical resistivity of diamond is not a problem for electrochemical measurements as long as relatively low scan rates (<100 mV/s) and low analyte concentrations (<1 mM) are employed.

Results from this and prior work have also revealed that the optical properties of the diamond OTE are stable during

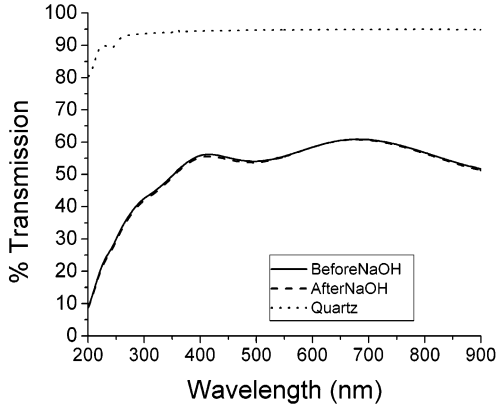


**Figure 1.** UV−vis transmission spectra for a diamond/quartz OTE before and after a 48 h exposure to 1 M NaOH. The spectrum for bare quartz is shown for comparison.

exposure of a variety of organic solvents (hexane, toluene, methanol, and dichloromethane) and aggressive aqueous solutions (1 M $HNO_3$ and 1 M NaOH).[6] As an example, transmission spectra before and after soaking a film in 1 M NaOH are presented in Figure 1. The spectrum for uncoated quartz is also shown, for comparison. The transparency of diamond in the visible region is ca. 55% and is lower than that for ITO, which is ca. 85%. In comparison, the optical properties of ITO were unchanged after exposure to hexane, toluene, or methanol. However, they were significantly affected during exposure to dichloromethane because of the isolated film dissolution. Significant film degradation and removal were also seen for 1 M $HNO_3$ and 1 M NaOH. This dissolution and film removal resulted in an increase in the optical transparency below 300 nm (i.e., the transparency approached that of the quartz substrate).

The majority of the light loss for diamond, particular at wavelengths less than 300 nm and greater than 700 nm, is due to absorbance by nitrogen impurities and by the boron dopant impurity band, respectively.[6,8] Reflection is the main light loss mechanism between 300 and 700 nm because of diamond's relatively high refractive index (2.41 at 590 nm).[6,8] For example, the calculated intensity loss due to reflection for light perpendicularly incident upon the diamond/quartz OTE is 27%. The remainder of the light loss is attributed to a combination of scattering and absorption (e.g., low levels of $sp^2$-bonded carbon impurity in the films). This means that this transparency in the visible region is about the best that can be achieved for diamond, even with the relatively high boron-doping level. By way of comparison, the transparency of a piece of polished white diamond (i.e., optically clear and free-standing) is only about 65% in this region. Though not as transparent as ITO, which would be a limitation for some electrooptical applications, the throughput is more than adequate for quality spectroelectrochemical measurements to be made.[5−8] Difference measurements are commonly made to improve the signal-to-noise ratios for an analyte, and a most important electrode requirement for such measurements is stable optical properties. Like the electrical properties, the optical properties were reproducible from diamond film-to-film.

**Anodic and Cathodic Polarization Tests.** The stabilities of the electrical and optical, as well as the electrochemical,

(14) Terzini, E.; Thilakan, P.; Minarini, C. *Mater. Sci. Eng.* **2000**, *B77*, 110.
(15) Liu, C.; Matsutani, T.; Asanuma, T.; Kiuchi, M. *Nucl. Instrum. Methods Phys. Res., Sect. B* **2003**, *206*, 348.
(16) Vaufrey, D.; Khalifa, M. B.; Tardy, J.; Ghica, C.; Blanchin, M. G.; Sandu, C.; Roger, J. A. *Semicond. Sci. Technol.* **2003**, *18*, 253.
(17) Donley, C.; Dunphy, D.; Paine, D.; Carter, C.; Nebesny, K.; Lee, P.; Alloway, D.; Armstrong, N. R. *Langmuir* **2002**, *18*, 450.
(18) Gheeraert, E.; Gonon, P.; Deneuville, A.; Abello, L.; Lucazeau, G. *Diamond Relat. Mater.* **1993**, *2*, 742.
(19) Show, Y.; Matsukawa, T.; Ito, H.; Iwase, M.; Izumi, T. *Diamond Relat. Mater.* **2000**, *9*, 337.
(20) Deneuville, A. In *Thin-Film Diamond I*; Nebel, C. E., Ristein, J., Eds.; Elsevier Inc.: Amsterdam, 2003; p 183.

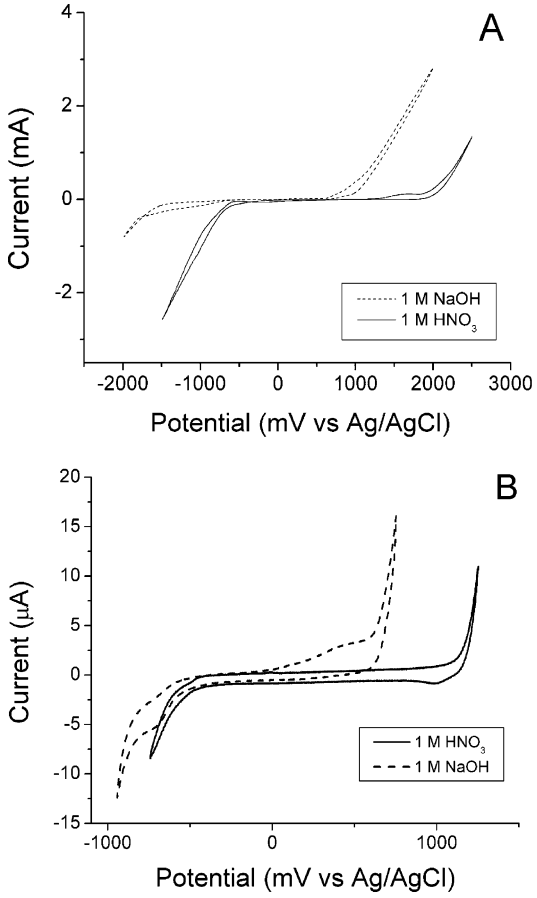


**Figure 2.** (A) Cyclic voltammetric $i-E$ curves for a diamond/quartz OTE in 1 M $HNO_3$ and 1 M NaOH at 25 mV/s. (B) Same voltammetric curves shown on an expanded current scale. Electrode area = 0.2 $cm^2$.

properties of the diamond OTE were evaluated before and after anodic and cathodic polarization. The conditions used herein were more severe (wider potential range and higher currents) than those used in earlier work.[6] Cyclic voltammetric $i-E$ curves for diamond in 1 M $HNO_3$ and 1 M NaOH are presented in Figure 2A. The $i-E$ curves are plotted with a reduced potential axis and a more sensitive current scale (3 orders of magnitude) in Figure 2B. The curves changed little in shape with cycle number and have more or less a featureless double layer region between the working potential limits. The magnitude of the anodic current at +100 mV (25 mV/s) is 1 $\mu$A. This value is in agreement with the background current previously reported for the diamond/quartz electrode but is a little larger than the typical current for a boron-doped diamond film deposited on Si.[6,11,21] The anodic potential limit at ca. 2000 mV in acid is characterized by oxygen evolution, and the cathodic limit at −700 mV is attributed primarily to hydrogen evolution. The maximum currents passed at the potential limits were ±1 mA (±5 mA/$cm^2$) or greater. The cathodic current at −700 mV may also contain a contribution from the reduction of dissolved oxygen, which is generated at the electrode surface during the positive-going sweep. The anodic potential limit at 1000 mV in alkaline medium is due to oxygen evolution, and the cathodic limit results from hydrogen evolution at −1500 mV. Again, there maybe some contribution from the reduction

(21) Granger, M. C.; Swain, G. M. *J. Electrochem. Soc.* **1999**, *146*, 4551.

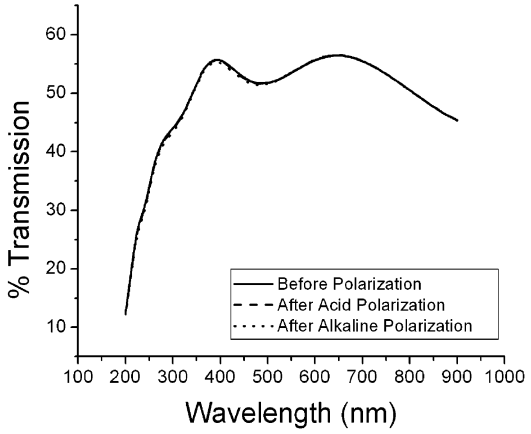


**Figure 3.** UV−vis transmission spectra for a diamond/quartz OTE before and after electrochemical polarization in both 1 M $HNO_3$ and 1 M NaOH. Cycling time = 2 h.

of dissolved oxygen generated on the forward sweep. Figure 2B reveals that some anodic current flows in NaOH above the capacitive background starting about 200 mV negative of the onset of oxygen evolution at 600 mV. During the reverse sweep, there is a cathodic peak at ca. −750 mV just prior to the hydrogen evolution current at −950 mV. Proof that this reduction current is linked with the anodic feature at ca. 400 mV is fact that the anodic current was not observed when the negative-going scan was reversed at −300 mV. These currents maybe associated with the oxidation and reduction of some carbon sites at the surface (i.e., formation of carbon−oxygen functional groups). Importantly, the optical and the electrical properties of the diamond OTE were unaffected during a 2 h period of potential cycling in either 1 M $HNO_3$ or 1 M NaOH. The former is illustrated in the UV−vis transmission spectra presented in Figure 3. In terms of the electrical properties, the nominal resistivity of the films was $9 \times 10^{-2}$ Ω cm before and after polarization in either medium. Similar stability was observed during shorter duration and less severe electrochemical polarization in these same media.[6]

In contrast, the electrical and optical properties of ITO were significantly altered during polarization in both 1 M $HNO_3$ and 1 M NaOH. Potential cycling was performed until electrical contact with the film was lost, which usually occurred within the first 20−30 cycles (∼1 h) in either medium. Clearly, chemical compositional and microstructural changes occur during the anodic and cathodic polarization of ITO and the changes produced extend into the film bulk.[13,17] It appears that most of the film degradation occurs during cathodic polarization. It is known, for example, that ITO can be irreversibly destroyed if the potential is poised in the hydrogen evolution regime for any extended period of time.[13] Results for potential cycling in 1M $HNO_3$ are shown in parts A and B of Figure 4. In Figure 4A, a series of cyclic voltammetric $i-E$ curves are shown between 2.5 and −1.0 V (25 mV/s) with the maximum current at the potential limits being ±1 mA (±5 mA/$cm^2$) or greater. The first 10 cycles are displayed. A wide working potential window is evident (ca. 2.8 V), similar to diamond. A cathodic peak of unknown origin is seen at ca. −300 mV between the oxygen and hydrogen evolution regimes. The presence

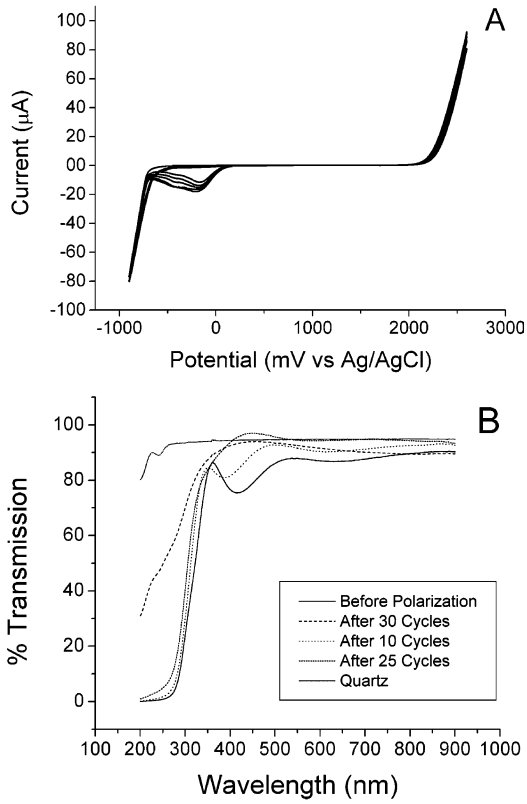


**Figure 4.** (A) Cyclic voltammetric $i-E$ curves for an ITO/quartz OTE in 1 M $HNO_3$ at 25 mV/s (cycle nos. 14−19). (B) Optical transmission spectra for the ITO/quartz OTE after potential cycling in 1 M $HNO_3$ at different times during the polarization.

of this peak suggests that some change in the chemical composition is occurring on the film surface and or in the bulk. It is supposed that this current is associated with the reduction of Sn(IV) oxide to Sn(II) or Sn. The electrical resistivity increased during polarization in both media to an unmeasurable value after cycling ($\sim 10^{-4}$ to >40 MΩ cm). The reduction of Sn(IV) would reduce the carrier concentration within the film causing an increase in the electrical resistivity. The potential cycling might also cause some roughening and disordering of the crystalline ITO, which would also lead to an increase in the electrical resitivity.[14,15] Evidence for surface roughening is provided in the ECAFM data presented below. The localized dissolution also contributes to the loss of electrical connectivity as well as the optical transparency increase. The spectra presented in Figure 4B provide evidence for the film loss as the optical transparency in the region below 300 nm increases with potential cycling.

Similar film degradation was also seen for ITO after polarization in 1 M NaOH. During potential cycling, a cathodic peak was seen at ca. −1600 mV, just prior to the onset potential for hydrogen evolution, along with a sharp oxidation peak at −1100 mV. Current crossover was seen in the voltammetric trace consistent with a activated process, such as the nucleation and growth of a metal deposit followed by its oxidation. The presence of these peaks is consistent with the some form of chemical change within the film. A big change in the optical properties was also seen after 10 cycles. Instead of film loss, deposition of opaque material was observed. As a consequence, the light throughput in the visible region decreased from ca. 85% to 20% or less. These deposits are likely metal or metal hydroxides of Sn and or In that form during the cathodic polarization. This deposited material did not adhere strongly to the film surface as it could be easily rinsed away with a stream of ultrapure water.

**Electrochemical Atomic Force Microscopy (EC-AFM).** Electrochemical AFM was used to probe for morphological changes in the diamond and ITO OTE's induced by the electrochemical polarization. The top row of AFM images in Figure 5 compares the same diamond OTE surface before polarization (left), after 12 potential cycles in 1 M $HNO_3$ (center), and 12 potential cycles in 1 M NaOH (right). Potential cycling in both media was from −2.5 to +2.5 V vs AgQRE (100 mV/s) with maximum current densities ≥1 mA/cm$^2$, and all images shown were recorded at 0 V. During polarization, the tip was disengaged from the surface due to extensive gas evolution. The images reveal that no detectable changes in the surface morphology occurred during polarization in either medium. Similar results were seen for longer duration cycling. The rms surface roughness was 17 nm over the 1 $\mu$m$^2$ area before cycling, 17 nm after cycling in $HNO_3$, and 16 nm after cycling in NaOH. The absence of morphological changes is consistent with diamond's stable electrical and optical properties, as discussed above.

In contrast, the morphology of ITO was degraded during the same polarizations. Representative images are shown in the bottom row of Figure 5. Images are shown for the surface before polarization (left), after potential cycling in 1 M $HNO_3$ (center), and after potential cycling in 1 M NaOH (right). Prior to polarization, a relatively smooth and continuous film exists. The film is composed of grains ca. 100 nm in diameter and has an rms surface roughness of 3 nm over the 1 $\mu$m$^2$ area. The grain size and surface roughness of this ITO film is greater than other films reported on in the literature.[17] After 30 potential cycles in 1 M $HNO_3$ between +2.0 and −0.8 V (a narrower potential range than for diamond), significant roughening develops. The nodular features remain about 100 nm in diameter but the nominal height increases to ca. 70 nm. Consequently, the rms surface roughness increases from 3 to 17 nm. This roughening is believed to be caused by film dissolution predominately at the boundaries between the grains. This dissolution is consistent with both the loss of electrical conductivity and the increase in optical transparency, as described above. After the 30th cycle in 1 M $HNO_3$, the electrode current decreased to zero as degradation occurred to the extent that lateral connectivity within the film was lost.

More significant morphological changes were observed for ITO during polarization in 1 M NaOH. The film was exposed to 20 potential cycles between −1.1 and + 0.3 V (a more narrow potential range than for diamond). The positive potential limit did not exceed +0.3 V to ensure that any cathodic current observed was attributable to reduction of species in the ITO film and not to the reduction of oxygen generated during the positive-going scan. Quite severe roughening is evident, which confirms that the degradation is caused by the cathodic polarization. The grains possess a distribution of diameters with many being larger than 200 nm. The surface roughness increases from 3 to 43 nm. The

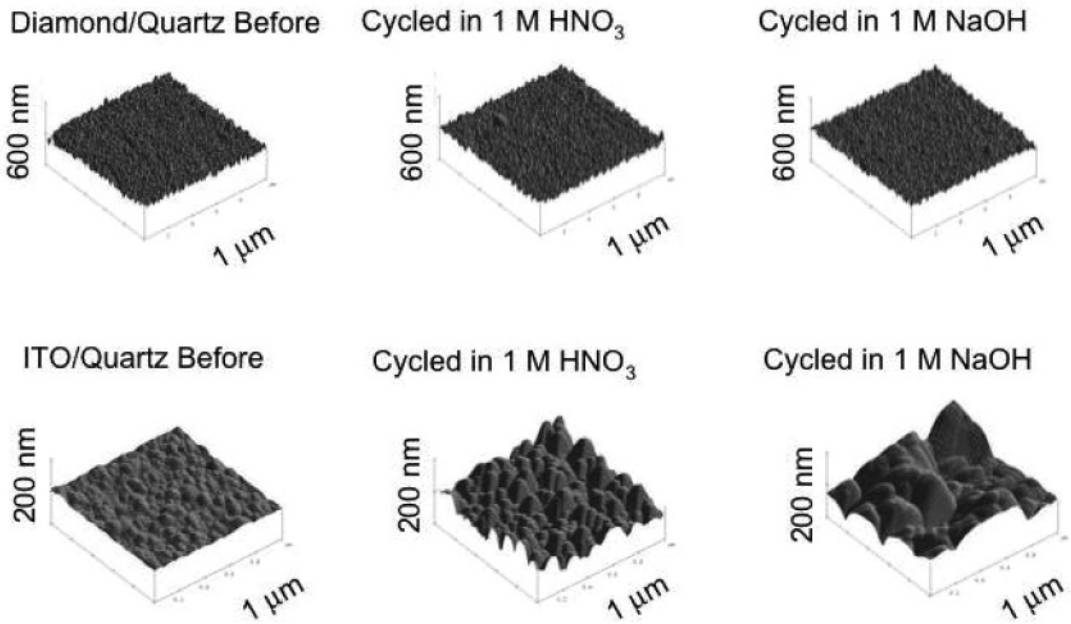


**Figure 5.** Electrochemical AFM images of a diamond/quartz (top row) and an ITO/quartz OTE (bottom row) at 0 V vs AgQRE. In each row, height mode images are presented for the untreated electrode (left), after electrochemical polarization in 1 M $HNO_3$ (center), and after electrochemical polarization in 1 M NaOH (right).

specific mechanisms of ITO degradation during potential cycling in acidic and alkaline media remain to be determined from further investigation.

**Conductivity-Probe AFM.** It has been shown that the electrical properties of the diamond OTE are quite stable, but it is important to know how uniform they are across a film. To answer this question, conductivity-probe AFM (CP-AFM) was utilized to spatially probe the electrical properties. This technique simultaneously produces a topographical image and a conductivity map of the surface. This technique has recently been employed for the first time to characterize the electrical properties of boron-doped diamond thin films deposited on conducting Si. Wang et al.[22] and Holt et al.[23] have found that the polycrystalline thin film consists of highly conducting zones isolated from one another by more insulating regions. In other words, the electrical properties appear inhomogeneous across the surface. In general, the "hot spots" were larger in dimension than any one grain and the surrounding grain boundary. It has also been observed that the fraction of the surface that is highly conducting increases with the boron doping level.[22,23] A topographical image (A) and a conductivity map (B) for a diamond OTE deposited for 1 h using a 10 ppm $B_2H_6$ source gas concentration are presented in Figure 6. Figure 6A reveals that the relatively smooth diamond surface has a nodular morphology with 25−50 nm feature sizes.[6] The bright regions in Figure 6B represent areas of higher electrical conductivity and the dark regions areas of lower conductivity. The *z*-axis voltage scale in Figure 5B is related to the current flowing between the film and tip. Using the gain of the current−voltage converter (3.3 $\mu$A/V), the current ranges from 0 to 33 $\mu$A. Given the +2 V bias between the tip and the film (which means current is flowing from the film into the tip), the light areas possess an apparent resistance of less than ca. 60 kΩ. When the conductivity map is compared with the topographical image, it is clear that some of the conductive zones are associated with boundaries between the nodular features. It appears that roughly 50% of the film

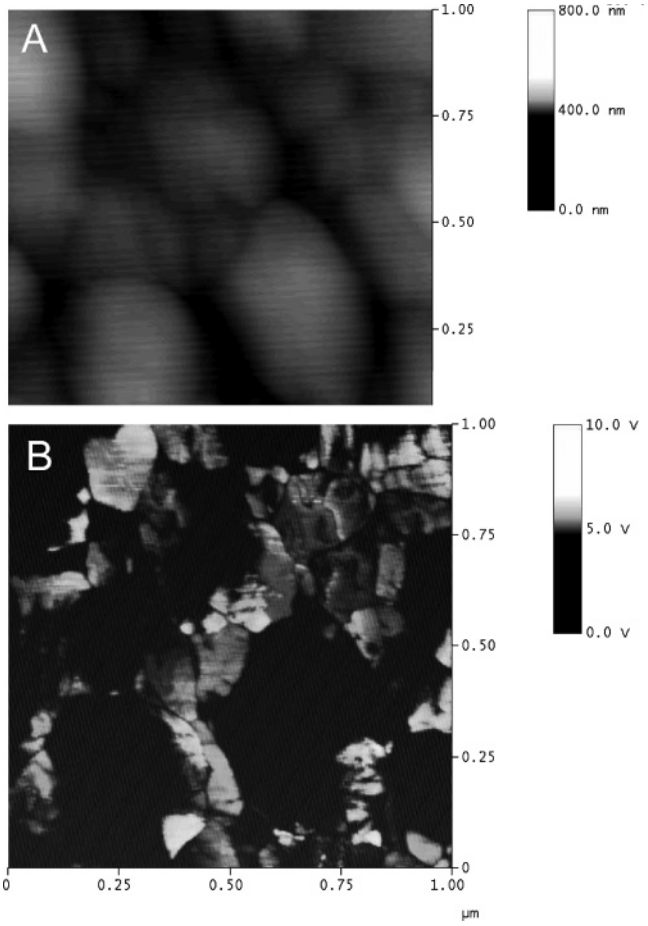


**Figure 6.** (A) Height mode image and (B) conductivity map for a diamond/quartz OTE obtained by conductivity-probe AFM.

(22) Wang, S.; Swain, G. M. Unpublished results.
(23) Holt, K. B.; Bard, A. J.; Show, Y.; Swain, G. M. *J. Phys. Chem. B* **2004**, *108*, 15117.

exhibits high conductivity. This has importance for the electrochemical measurements because the more highly conducting regions are the locations where the fastest rate of electron-transfer is expected.[24] It is important to remember, though, that the current in this measurement is flowing laterally through the film with one contact point being between the tip and film and the other being the film edge or corner. Therefore, a high resistance site might appear so not because the region is devoid of charge carriers but rather because of poor lateral connectivity (i.e., carrier mobility) with other regions of the film.

More work is needed to conclusively determine the origins of the inhomogeneous electrical conductivity, but there are at least three possible causes to consider. First, it is well-known that boron-doping of polycrystalline diamond occurs inhomogeneously, depending on the growth sector, and this leads to a variable charge carrier concentration across the surface.[25,26] Second hydrogen can be incorporated into the film during deposition or hydrogen plasma treatment and function as a donor and compensate boron acceptor sites or as an acceptor and increase the charge carrier concentration.[27−29] The local concentration of lattice hydrogen could be variable as could its compensating interactions with boron acceptors across the surface. Third, isolated regions of a film might simply possess poor lateral connectivity with other regions of the film (i.e., grain boundary contact). In this case, the poor conductivity would result from low carrier mobility.

**Electrochemical Activity.** The electrochemical activity of the diamond OTE was evaluated before and after polarization in acidic and alkaline media using two redox systems: $Ru(NH_3)_6^{3+/2+}$ and $Fe(CN)_6^{4-/3-}$. A cyclic voltammetric $i-E$ curve for 0.1 mM $Ru(NH_3)_6^{3+/2+}$ in 1 M KCl showed nearly reversible electron-transfer kinetics with a $\Delta E_p$ of 62 mV (100 mV/s). After sequential polarization for 1 h each in 1 M $HNO_3$ and 1 M NaOH (25 mV/s), $\Delta E_p$ was unchanged at 62 mV. The potential limits of the cycling were the same as those listed above with maximum currents of $\pm 1$ mA ($\pm 5$ mA/cm$^2$). The peak potential separation was observed to increase with scan rate consistent with quasi-reversible electron-transfer kinetics. The reaction rate was limited by semi-infinite linear diffusion as the reduction peak current scaled proportionally with the square root of the potential sweep rate ($R^2 \geq 0.99$) both before and after cycling. The heterogeneous electron-transfer rate constant for this redox couple is known to be relatively insensitive to the surface cleanliness, surface microstructure, and surface chemistry of both diamond and sp$^2$ carbon electrodes.[11,30−34] It is most sensitive to the density of electronic states at the electrode surface that are available for charge transfer. The low and unchanging $\Delta E_p$ indicates that (i) the film possesses sufficient electrical conductivity, albeit in an apparent inhomogeneous fashion, to support relatively rapid electron transfer, and (ii) the electrochemical properties of the diamond OTE, at least toward this redox system, are stable even after extended potential cycling in acidic and alkaline media. The stability of the electrochemical properties is directly related to the stability of the electrical properties.

Cyclic voltammetric $i-E$ curves for 0.1 mM $Fe(CN)_6^{3-/4-}$ in 1 M KCl before polarization had a $\Delta E_p$ of 86 mV (100 mV/s) with the oxidation peak current that varyied linearly with the square root of the scan rate ($R^2 \geq 0.98$). After sequential polarizations for 1 h in 1 M $HNO_3$ and 1 M NaOH (25 mV/s), $\Delta E_p$ was relatively unchanged at 81 mV. Again, this relatively unchanged value is consistent with the stable electrical properties. The surface chemistry was, however, likely altered during the polarization being converted from a hydrogen to an oxygen termination.[21] While the heterogeneous electron-transfer rate constant for $Ru(NH_3)_6^{3+/2+}$ is relatively insensitive to the presence of surface oxygen, the rate constant for $Fe(CN)_6^{3-/3-}$ is. For diamond, surface oxygen generally decreases the rate constant for reasons that remain unclear.[21] The fact that $\Delta E_p$ did not change suggests that little surface oxygen was incorporated during the polarization at the sites where electron-transfer is occurring.

## Conclusion

Several conclusions can be reached regarding the electrical, optical, and electrochemical properties of the diamond OTE, in comparison with ITO.

(i) Diamond thin film on quartz can be prepared with reproducible electrical, optical, and electrochemical properties.

(ii) The electrical and optical properties of diamond are stable during exposure to wide range organic solvents and aggressive aqueous solutions. Severe film degradation of ITO occurred during exposure to dichloromethane, 1 M $HNO_3$, and 1 M NaOH.

(iii) Diamond is not as electrically conducting as is ITO (ca. $10^{-2}$ vs $10^{-5}$ $\Omega$ cm) and is not as optically transparent (55 vs 85% transparency in the visible region). The higher resistivity is attributed to a lower carrier mobility in the nanograined diamond thin film. These are drawbacks for application of this new OTE in electrooptical devices. However, the higher electrical resistivity and lower transparency of diamond are not limitations for difference spectroelectrochemical measurements (in a thin layer cell) as long as relatively low scan rates ($<100$ mV/s) and low analyte concentrations ($\leq 0.1$ mM) are employed.

(iv) The electrical, optical, and electrochemical properties of diamond are stable during anodic and cathodic polarization in 1 M $HNO_3$ and 1 M NaOH at current densities up to $\pm 5$

(24) Whitworth, A. L.; Mandler, D.; Unwin, P. R. *Phys. Chem. Chem. Phys.* **2005**, *7*, 356.
(25) Kobashi, K.; Nishimura, K.; Kawate, Y.; Horiuchi, T. *Phys. Rev. B* **1988**, *38*, 4067.
(26) Ushizawa, K.; Watanabe, K.; Ando, T.; Sakaguchi, I.; Nishitani-Gamo, M.; Sato, Y.; Kanda, H. *Diamond Relat. Mater.* **1998**, *7*, 1719.
(27) Chevallier, J.; Theys, B.; Lusson, A.; Grattepain, C. *Phys. Rev. B* **1998**, *58*, 7966.
(28) Denisenko, A.; Aleksov, A.; Pribil, A.; Gluche, P.; Ebert, W.; Kohn, E. *Diamond Relat. Mater.* **2000**, *9*, 1138.
(29) Goss, J. P.; Jones, R.; Heggie, M. I.; Ewels, C. P.; Briddon, P. R.; Oberg, S. *Phys. Rev. B* **2002**, *65*, 115207−1.
(30) Show, Y.; Witek, M. A.; Sonthalia, P.; Swain, G. M. *Chem. Mater.* **2003**, *15*, 879.
(31) Fischer, A. E.; Show, Y.; Swain, G. M. *Anal. Chem.* **2004**, *76*, 2553.
(32) Chen, P.; McCreery, R. L. *Anal. Chem.* **1996**, *68*, 3958.
(33) Chen, P.; Fryling, M. A.; McCreery, R. L. *Anal. Chem.* **1995**, *67*, 3115.
(34) Rice, R. J.; McCreery, R. L. *Anal. Chem.* **1989**, *61*, 1637.

$mA/cm^2$. On the other hand, severe degradation of ITO occurs during polarization in either of these media. The degradation mostly occurs during cathodic polarization. ECAFM measurements confirmed the morphological stability of diamond and the localized film degradation of ITO.

(v) Diamond exhibits relatively rapid electron-transfer kinetics (i.e., low cyclic voltammetric $\Delta E_p$ values) for $Ru(NH_3)_6^{3+/2+}$ and $Fe(CN)_6^{3-/4-}$ without any conventional pretreatment, and the $\Delta E_p$ for these redox systems was unchanged after anodic and cathodic polarization.

(vi) CP-AFM measurements indicate the diamond film is not homogeneously conducting but rather consists of "hot spots" of high electrical conductivity.

**Acknowledgment.** This work was supported by grants from the National Science Foundation (CHE-9983676 and 0049090). The authors also thank Dr. David Young of NREL for his assistance with the optical reflection and Hall measurements on the diamond OTE.

CM050762Z